TRANSACTIONS
OF THE INSTITUTE OF
FLUID-FLOW MACHINERY

PRACE

INSTYTUTU MASZYN PRZEPŁYWOWYCH

101

DARIUSZ P. MIKIELEWICZ[1]

Modelling of an ascending flow of air in a heated vertical pipe[2]

The present work reports the results of numerical simulations, using four different $k \sim \epsilon$ turbulence models, of the experiments performed on buoyancy-influenced ascending flow of air in a heated vertical tube. The calculations have been performed using a variable property formulation of the governing equations. The simulations have been performed using a constant value of the turbulent Prandtl number of 0.85. Of the models considered it has been found that the Sato, Shimada and Nagano and Launder and Sharma models are performing well under conditions described by the experimental data. However, these models are still not reliable enough to be recommended for the modelling of the buoyancy-influenced flows.

Nomenclature

B	– buoyancy parameter, $Gr/(Re^{3.425}Pr^{0.8})$,	r, z	– cylindrical polar coordinates,
C_p	– specific heat capacity at constant pressure,	R_k	– turbulence Reynolds number $yk^{1/2}/\nu$,
C_1, C_2	– constants in modelled dissipation equation,	Re	– Reynolds number, $\rho W_b D/\mu$,
C_μ	– constant in constitutive equation of eddy viscosity model,	Re_t	– turbulence Reynolds number, $k^2/\nu\epsilon$,
D	– term in low-Reynolds-number k-equation, pipe diameter,	T	– temperature, °C,
E	– term in low-Reynolds-number ϵ-equation,	V, W	– mean velocity in r, z directions,
f_1, f_2	– functions in dissipation equation,	y	– dimensional distance from the wall,
f_μ	– function in constitutive equation of $k \sim \epsilon$ model,	y^+	– non-dimensional distance from the wall,
g	– acceleration due to gravity,	y^*	– turbulence parameter in AKN model, $y/\nu(\nu\epsilon)^{0.25}$,
Gr	– Grashof number, $\beta g D^4 q/\lambda\nu^2$,	ϵ	– rate of dissipation of turbulence kinetic energy,
i	– enthalpy,	λ	– thermal conductivity,
k	– turbulence kinetic energy,	μ	– dynamic viscosity,
Nu	– Nusselt number, $qD/(T_w - T_b)\lambda$,	ν	– kinematic viscosity,
p	– pressure,	ρ	– density,
Pr	– Prandtl number, $C_p\mu/\lambda$,	σ_t	– turbulent Prandtl number,
q	– wall heat flux,	$\sigma_k, \sigma_\epsilon$	– turbulent Prandtl number for diffusion of k, ϵ.

[1]Institute of Fluid-Flow Machinery, Department of Thermodynamics and Heat Transfer, ul. Fiszera 14, 80-952 Gdańsk

Present address: Technical University of Gdańsk, Heat Technology Department, Narutowicza 11/12, 80-952 Gdańsk

<div align="center">Subscripts</div>

b –	bulk,	YS –	Yang and Shih low-Reynolds-number $k \sim \epsilon$ model [6],
cp –	constant property forced convection,		
in –	refers to bulk inlet conditions,	AKN –	Abe, Kondoh and Nagano low-Reynolds--number $k \sim \epsilon$ model [7],
t –	turbulent,		
vp –	variable property forced convection,	SSN –	Sato, Shimada and Nagano low-Reynols--number $k \sim \epsilon$ model [8],
w –	wall,		
LS –	Launder and Sharma low-Reynolds--number $k \sim \epsilon$ model [5],	EXP –	experimenal data due to Vilemas, Poskas and Kaupas [1].

1. Introduction

In recent years, there has been a great concentration of effort in industry on computational modelling of problems involving turbulent fluid flow and heat transfer, usually using codes of considerable versatility. It is sometimes mistakenly assumed that the turbulence models incorporated in such codes possess more universality than is the case and this can lead to incorrect usage of the codes and wrong conclusions being drawn from the results obtained. The comprehensive set of experimental results on buoyancy-influenced heat transfer for ascending flow of air in a vertical tube, reported recently by Vilemas et al. [1], represent a very significant addition to the surprisingly sparse amount of data previously available. This mode of convection involves the progressive impairment of heat transfer with build-up of buoyancy influence, leading to a minimum level where the flow is laminarized. This is followed, with a further increase of buoyancy influence by recovery and the eventual enhancement of heat transfer (in relative terms). The picture is usually clouded by the influence of the variable property effects.

In the study reported here, direct comparisons were made between the experimental data and simulations performed using several models from the $k \sim \epsilon$ family of turbulence models. The work is intended to show the up to date capability of the $k \sim \epsilon$ models to predict axisymmetric, parabolic, two-dimensional ascending flow of air in a vertical pipe with the account of the variation of physical properties. The work is an extension of the work [2], where several other models of turbulence have been implemented in the computer code CONVERT originally developed by Cotton [3] and Yu [4]. As a rather unsatisfactory result has been achieved from these studies, the author embarked on the further examination of the $k \sim \epsilon$ models in search of other, more adequate near-wall parameters, which would better respond in wall-bounded shear flows to the influences such as severe pressure gradient. Further models have been collected, which only appeared in the literature very recently. These models have been developed on the basis of different parameters which are responsible for turbulence characteristics in the near-wall region, where most of diffusion of turbulence takes place. The models selected for the study were: LS (Launder and Sharma [5]), YS (Yang and Shih [6]), AKN (Abe, Kondoh and Nagano [7]) and SSN (Sato, Shimada and Nagano

[8]). The results of numerical simulations are directly compared with the experimental data of Vilemas et al. [1] on ascending flow of air in the heated vertical pipe.

2. Governing equations

Since the geometry considered here is the pipe flow, the governing equations are written in the 'boundary layer' approximation. The principal flow direction coincides with the axis of the pipe and the main gradients are in the direction normal to the axis. The thermal boundary condition of a uniform wall heat flux applies. The equations are as follows:

Continuity equation:

$$\frac{1}{r}\frac{\partial(\rho r V)}{\partial r} + \frac{\partial(\rho W)}{\partial z} = 0. \tag{1}$$

Momentum equation:

$$\frac{1}{r}\frac{\partial(\rho r V W)}{\partial r} + \frac{\partial(\rho W^2)}{\partial z} = -\frac{dp}{dz} + \frac{1}{r}\frac{\partial}{\partial r}\left[r(\mu + \mu_t)\frac{\partial W}{\partial r}\right] + \rho g. \tag{2}$$

Energy equation:

$$\frac{1}{r}\frac{\partial(r\rho V h)}{\partial r} + \frac{\partial(\rho W h)}{\partial z} = \frac{1}{r}\frac{\partial}{\partial r}\left[r\left(\frac{\lambda}{C_p} + \frac{\mu_t}{\sigma_t}\right)\frac{\partial h}{\partial r}\right]. \tag{3}$$

After [9], the turbulent Prandtl number has been assigned a uniform value of 0.85.

3. Turbulence models

In order to solve the above equations the concept of turbulent viscosity is employed. In the case of the $k \sim \epsilon$ models the velocity scale is represented by the square root of the turbulence kinetic energy k and the turbulence length scale is the product of its rate of dissipation ϵ ($= k^{\frac{3}{2}}/\epsilon$). In low-Reynolds-number models, which are considered here, the transport equations are solved over the entire flow domain without recourse to wall functions. This approach proved to be successful in the simulations of buoyancy-influenced wall shear flows in the papers of Cotton and Jackson [10,11], where the turbulence model of Launder and Sharma [5] was used to simulate experimental data [12-14]. Generally, a viscosity model can be written as:

$$\mu_t = C_\mu f_\mu \frac{\rho k^2}{\tilde{\epsilon}}. \tag{4}$$

The equations, which define transport of k and ϵ equations are as follows:
k-transport

$$\frac{1}{r}\frac{\partial(\rho r V k)}{\partial r} + \frac{\partial(\rho W k)}{\partial z} = \mu_t\left(\frac{\partial W}{\partial r}\right)^2 + \frac{1}{r}\frac{\partial}{\partial r}\left[r\left(\mu + \frac{\mu_t}{\sigma_k}\right)\frac{\partial k}{\partial r}\right] - \rho(\epsilon), \quad (5)$$

ϵ-transport

$$\frac{1}{r}\frac{\partial(\rho r V \tilde{\epsilon})}{\partial r} + \frac{\partial(\rho W \tilde{\epsilon})}{\partial z} =$$

$$= C_1 f_1 \frac{\tilde{\epsilon}}{k}\mu_t\left(\frac{\partial W}{\partial r}\right)^2 + \frac{1}{r}\frac{\partial}{\partial r}\left[r\left(\mu + \frac{\mu_t}{\sigma_\epsilon}\right)\frac{\partial \tilde{\epsilon}}{\partial r}\right] - C_2 f_2 \frac{\rho\tilde{\epsilon}^2}{k} + \rho E, \quad (6)$$

$$\tilde{\epsilon} = \epsilon - D. \quad (7)$$

The various models differ by the use of different functions f_μ, f_1, f_2 and also different terms D and E. In eddy viscosity model, coefficient C_μ is a constant, while f_μ is a damping function reducing the eddy viscosity near the wall. Some models use as a turbulence time scale k/ϵ and solve an equation for ϵ itself (YS, AKN models). In other models, the turbulence time scale is defined by the ratio $k/\tilde{\epsilon}$ assuming that the value of $\tilde{\epsilon}$ is equal to zero at the wall (LS, SSN models). The function f_2 in the ϵ-equation is usually effective only very close to the wall. It is introduced to simulate the change in the decay rate of homogeneous turbulence as the turbulent Reynolds number becomes small. The extra term E is introduced to increase the production of ϵ near the wall. All the models considered have the form that when f_μ and f_2 are set to unity, and terms D and E are set to zero, the standard high-Reynolds version of the $k \sim \epsilon$ model is retrieved.

In [2], from the models considered there, it has been found that only wall functions implemented in the Launder and Sharma model were capable to capture changes taking place in mixed convection with variable properties. The other models tested here (YS, AKN and SSN), which have not been examined by the author earlier, implement either different parameters in near-wall damping functions (AKN model) or are better adjusted to the experimental data (YS and SSN models) (at least the authors say so). Especially interesting are the parameters employed by the AKN model which are different from the others and employ Kolmogorov velocity scale $u_\epsilon = (\nu\epsilon)^{1/4}$.

Tables 1-3 present details of functions and constants incorporated in the different formulations of the $k \sim \epsilon$ models used. In the below tables various definitions of the turbulent Reynolds number are used. These are: $Re_t = k^2/\nu\epsilon$, $R_k = yk^{\frac{1}{2}}/\nu$, $y^* = y/\nu(\nu\epsilon)^{0.25}$.

4. Results

Firstly, the performance of the models, when used to simulate turbulent flow and heat transfer in pipes under conditions of constant properties forced convection is reported. In Table 4, the model predictions are compared with the

Table 1. Damping functions used in various $k \sim \epsilon$ models

Model	f_1	f_2	f_μ
LS	1.0	$1 - 0.3 \exp(-Re_t^2)$	$\exp[-3.4/(1 + Re_t/50)^2$
YS	$\dfrac{Re_t^{1/2}}{1 + Re_t^{1/2}}$	$\dfrac{Re_t^{1/2}}{1 + Re_t^{1/2}}$	$\dfrac{[1 - \exp(-aR_k^{1/4} - bR_k^{1/2} - cRe_k)]^{0.5}}{(1 + 1/\sqrt{Re_t})}$ $a = 1.5 \cdot 10^{-4}, \ b = 5 \cdot 10^7, \ c = 1 \cdot 10^{-10}$
AKN	1.0	$[1 - \exp(-y^*/3.1)]^2 \times$ $\times \{1 - 0.3 \exp[-(Re_t/6.5)^2]\}$	$[1 - \exp(-y^*/14)]^2 \times$ $\times \{1 + 5/Re_t^{0.75} \exp[-(Re_t/200)^2]\}$
SSN	1.0	$1 - 0.3 \exp[-(Re_t/6.5)^2]$	$1 - \exp(Re_t/90) \times$ $\times \{1 + (7/Re_t) \exp[-\sqrt{Re_t/10}]\}$

empirical correlation equation of Kurganov-Petukhov [15], which provides probably the most reliable description available on constant property developing forced convection in pipes. In the calculations, the hydrodynamically fully developed profiles of velocity, turbulent kinetic energy and dissipation rate were first obtained and the fully developed Nusselt number then calculated. The calculations started with approximate, theoretical initial profiles and the code ran for 100 diameters in order to ensure that a fully developed fluid flow condition has been reached. Table 4 shows the values of forced convection Nusselt number obtained in the simulations along with those given by the Kurganov-Petukhov correlation for fully developed constant property forced convection. The range of Reynolds number considered is from $4.5 \cdot 10^3$ to $6 \cdot 10^4$.

There are discrepancies between the values yielded by the various models and the correlation equation but the percentage differences are generally quite small. The majority of models predict Nusselt numbers which agree with the correlation estimates within 5%. However, a larger discrepancy is found in the case of the YS model which overpredicts heat transfer coefficient by as much as 11%. The generally good agreement between the model calculations and correlation stems partly from the fact, that constants used in the models were originally adjusted to fit data for air flows. For such a fluid the thermal layer is of comparable thickness to the hydrodynamic layer and as a consequence the results are less sensitive to the precise specification of near-wall turbulence, than in the case of liquids such as water for which the thermal layer is much thinner [16].

Next, attention was focused on the influences of the temperature dependence of physical properties. For air, the density decreases with the increase of temperature and viscosity, conductivity and specific heat all increase with the increase of temperature. As the variations of density and dynamic viscosity are in opposite directions, the kinematic viscosity decreases strongly with temperature. This has a direct effect on near-wall damping through the local turbulent Reynolds

Table 2. Model terms in various $k \sim \epsilon$ models

Model	D	E
LS	$2\mu(\partial\sqrt{k}/\partial y)^2 \quad y^+ \leq 2$ $2\mu k/y^2 \qquad\quad y^+ > 2$	$\frac{2\mu\mu_t}{\rho}\left(\frac{\partial^2 W}{\partial y^2}\right)^2$
YS	0	$\frac{\mu\mu_t}{\rho}\left(\frac{\partial^2 W}{\partial y^2}\right)^2$
AKN	0	0
SSN	0	$\exp\left[-\left(\frac{y^+}{37}\right)^2\right]\frac{\mu\mu_t}{\rho}\left(\frac{\partial^2 W}{\partial y^2}\right)^2$

The boundary conditions used in the solution of the k and $\check{\epsilon}$ equations are as follows:

$k = 0$ for all models,

$\check{\epsilon} = 0$ for LS and SSN,

$\epsilon_w = 2\mu(\partial k^{1/2}/\partial y)^2$ for YS and AKN.

number. The influences of variable properties can take two distinct forms, one stemming from buoyancy forces which arise as a consequence of non-uniformity of density and the other from both axial and radial variations of the transport properties viscosity and thermal conductivity. In the case of air, the Reynolds number decreases axially as a result of increase in dynamic viscosity. The Prandtl number remains virtually constant. The Nusselt number is directly dependent on Reynolds number and as a result, the Nusselt number falls axially. These changes are successfully captured by various empirical correlations if local values of bulk temperature are used in evaluating the physical properties in Reynolds and

Table 3. Model constants in various $k \sim \epsilon$ models

Model	C_μ	C_1	C_2	σ_k	σ_ϵ
LS	0.09	1.44	1.92	1.0	1.3
YS	0.09	1.44	1.92	1.0	1.3
AKN	0.09	1.50	1.90	1.4	1.4
SSN	0.09	1.45	1.90	$\frac{1.2}{1 + 3.5\exp(-Re_t/100)}$	$\frac{1.2}{1 + 3.5\exp(-Re_t/100)}$

Table 4. Fully developed constant property Nusselt number for air; $Pr = 0.706$, $Pr_t = 0.85$

Model	Reynolds number						
	5000	7500	10000	20000	30000	40000	60000
LS	17.059	23.538	29.995	51.862	71.551	89.997	124.55
YS	20.773	28.091	35.143	59.465	81.212	101.51	139.39
AKN	19.731	26.909	34.295	58.235	79.663	99.639	136.86
SSN	17.856	24.046	30.094	51.246	70.357	88.256	121.75
KURGANOV PETUKHOV	17.224	24.062	30.289	52.044	71.171	88.862	121.60

Prandtl number. The radial effect is usually accounted for by a simple power law correction factor, in which the absolute temperature ratio is raised to some appropriate power. This is an appropriate approach, because the thermophysical properties can be related to temperature by simple power law relationships to a good degree of accuracy in the case of air. Thus, properties are evaluated at the local bulk temperature in the basic correlation equation and the variable property effect is accounted for by an additional term involving a ratio of the absolute temperature ratio raised to a suitable power. The equation representing variable property heat transfer can therefore be written in the form:

$$\frac{Nu}{Nu_{cp}} = \left(\frac{T_w}{T_b}\right)^n \qquad (8)$$

in which Nu_{cp} is the constant property Nusselt number and indices b and w refer to bulk and wall values respectively. A typical value quoted for the index n in the case of air is (-0.4) (see for example Barnes and Jackson [17]). It has been concluded from [2, 18] that the models considered here tend to overpredict the influence of variable properties. This conclusion has been arrived at based on water flow consideration, where the major contribution to the property variation comes from viscosity variation. This was the case especially for the LS model whereas the other models considered here did overpredict the effects but to a smaller extent.

Finally, we turn our attention to conditions where buoyancy-influences are present. A buoyancy parameter $(B = Gr/(Re^{3.425}Pr^{0.8}))$ of the kind proposed by Jackson and Hall [19-20] serves to quantify the influences of buoyancy. As it has been mentioned earlier, the data base on mixed convection for ascending flow in vertical tubes was recently extended greatly by the publication of a com-

Table 5. Conditions (at inlet) for the simulations of Vilemas, Poskas and Kaupas experiments

Series	Run	Re	$Gr \times 10^{-9}$	Pr	$B \times 10^6$	T_{in}
	1	19400	0.452	0.704	1.1875	20.19
	2	13300	0.239	0.706	2.3250	18.84
1	3	8850	0.184	0.704	7.3125	20.63
	4	6162	0.577	0.704	76.063	21.51
	5	19600	1.204	0.704	3.1625	21.12
	6	20700	2.389	0.704	5.0500	20.80
2	7	11400	1.576	0.704	26.150	20.72
	8	7822	1.380	0.704	81.613	20.62

prehensive set of results by Vilemas, Poskas and Kaupas (1992). Their data encompass a wide range of conditions from what is essentially forced convection covering the very sensitive region of impaired heat transfer and then extending into the region of enhanced heat transfer. Some cases involve small wall-to-bulk temperature differences ($T_w/T_b \approx 1.05 - 1.1$) and small bulk temperature rise ($\Delta T_b < 30°C$) but some of the remaining data is strongly influenced by variable properties ($T_w/T_b \approx 1.4 - 1.5, \Delta T_b < 200°C$).

Eight cases are presented here in two series of four. The first series involves small or moderate influences of variable properties, whereas in the second, the effects of variable properties are quite marked. The inlet Reynolds number varies from 6000 to 20000 and Grashof number is in the range from $4.5 \cdot 10^8$ to $1.4 \cdot 10^9$ The inlet buoyancy parameter varies from $1.19 \cdot 10^{-6}$ to $8.16 \cdot 10^{-4}$. Simulated results are presented in the form of wall temperature development and compared against experimental data from Vilemas et al. In these figures, the development of bulk temperature (same in the case of experiment and all simulations) is also given. Additionally, the ratio of Nusselt number in buoyancy-influenced case normalised by corresponding forced convection value (Nu_{fc}) is presented in terms of axial development. Table 5 gives details of the inlet bulk conditions.

Runs 1 to 4 This series is for conditions where the influences of variable properties are quite small. Therefore, as in the case of the simulations of the experiments of Carr et al. [12], the influence of buoyancy can be observed alone. The buoyancy parameter is in the range from $1.1875 \cdot 10^{-6}$ to $7.606 \cdot 10^{-5}$. These values cover
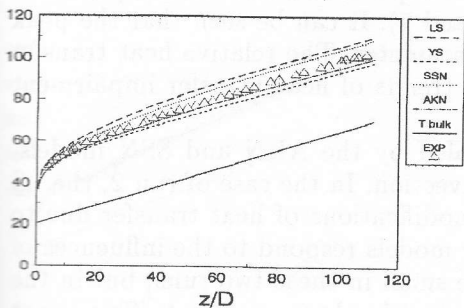
Fig. 1. Wall temperature development – simulation of Vilemas et al. experiment – run 1.
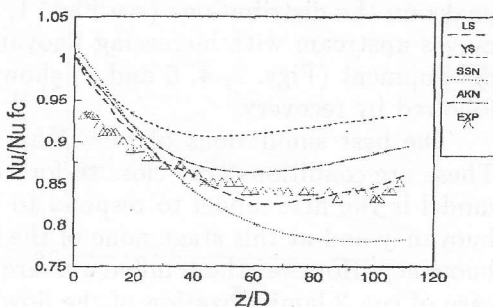
Fig. 2. Relative heat transfer development – run 1.
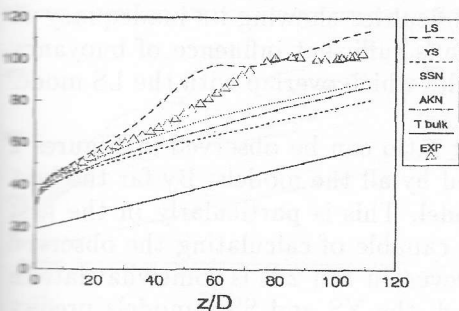
Fig. 3. Wall temperature development – simulation of experiment of Vilema et al. – run 2.
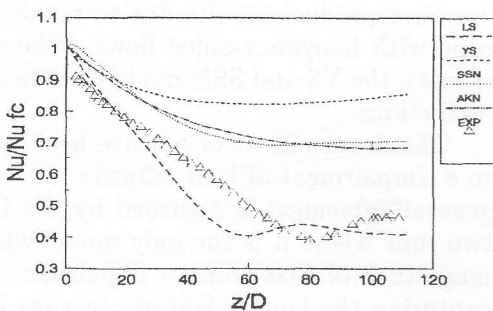
Fig. 4. Relative heat transfer development – run 2.
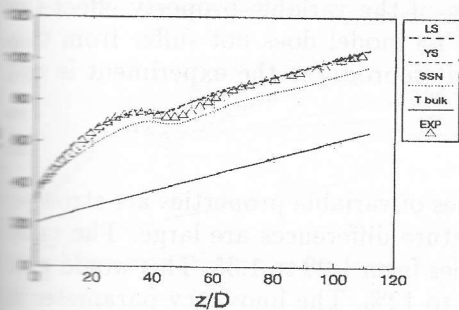
Fig. 5. Wall temperature development – simulation of experiment of Vilemas et al. – run 3.
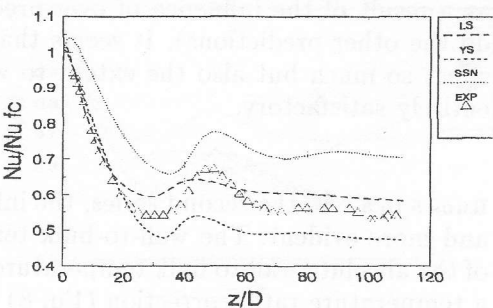
Fig. 6. Relative heat transfer development – run 3.

a wide range of buoyancy influences, from conditions where only small modification of heat transfer occurs, through the condition of maximum impairment and into the region where recovery of heat transfer takes place. With increase of the buoyancy parameter, the measured wall temperatures show development of peaks on the distributions (see Figs. 1, 3, 5 and 7). It can be seen that the peak moves upstream with increasing buoyancy parameter. The relative heat transfer development (Figs. 2, 4, 6 and 8) shows the trends of heat transfer impairment followed by recovery.

The best simulations of runs 1 are revealed by the AKN and SSN models. These are conditions very close to forced convection. In the case of run 2, the LS model is the first model to respond to the modifications of heat transfer due to buoyancy and at this stage none of the other models respond to the influences of buoyancy. However these influences are quite small in these two runs, but in the case of run 2 laminarization of the flow is evident in the experiment. This is not captured by any of the model simulations.

With increased influence of buoyancy (runs 3 and 4) remaining models, namely the YS and SSN models, start to respond more strongly. The AKN model does not produce results due to numerical difficulties showing its inadequacy to cope with buoyancy-aided flows. Where there is sufficient influence of buoyancy (run 4), the YS and SSN models produce results which overlap with the LS model predictions.

The development of relative heat transfer ratio can be observed in Figures 2 to 8. Impairment of heat transfer is calculated by all the models. By far the best general agreement is returned by the LS model. This is particularly in the first two runs where it is the only model which is capable of calculating the observed magnitude of heat transfer impairment. However, in run 2 it is somewhat late in capturing the laminarization. In runs 3 and 4, the YS and SSN models predict more or less the correct level of heat transfer impairment along with the LS model. In the last run of the series (run 4), enhancement of heat transfer is indicated in the experiment. The LS model calculations differ by some 15% from experiment as a result of the influence of over-prediction of the variable property effect (as do the other predictions). It seems that the YS model does not suffer from this effect so much but also the extent to which it reproduces the experiment is not entirely satisfactory.

Runs 5 to 8 In the second series, the influences of variable properties are stronger and more evident. The wall-to-bulk temperature differences are large. The ratio of the absolute wall to bulk temperatures varies from 1.28 to 1.35. This would give a temperature ratio correction (Eq. 8) of 10 to 12%. The buoyancy parameter is in the range $3.1625 \cdot 10^{-6}$ to $8.1613 \cdot 10^{-5}$. These conditions vary from those near maximum impairment into the enhanced region of heat transfer. Peaks on the wall temperature are present in all the data considered (see Figs. 9, 11, 13 and 15). With increase of buoyancy, an upstream shift of the peaks is evident. The non-uniformity of peaks increases with increase of the buoyancy parameter. The
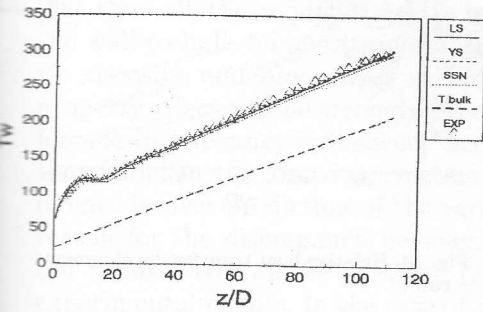
Fig. 7. Wall temperature development – simulation of experiment of Vilemas et al. – run 4.
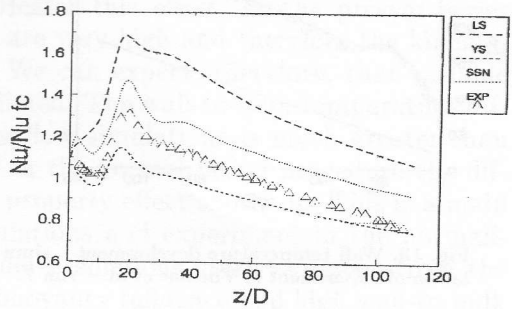
Fig. 8. Relative heat transfer development – run 4.
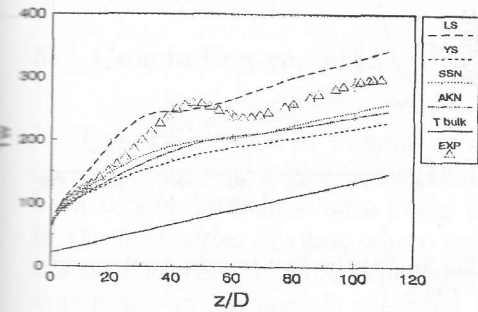
Fig. 9. Wall temperature development – simulation of experiment of Vilemas et al. – run 5.
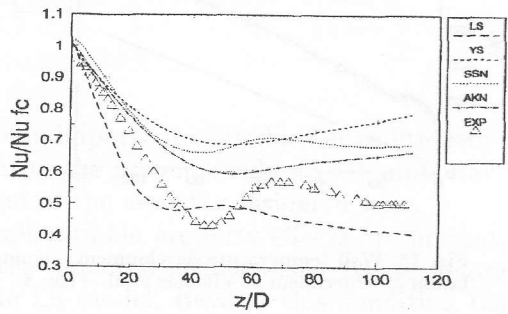
Fig. 10. Relative heat transfer development – run 5.
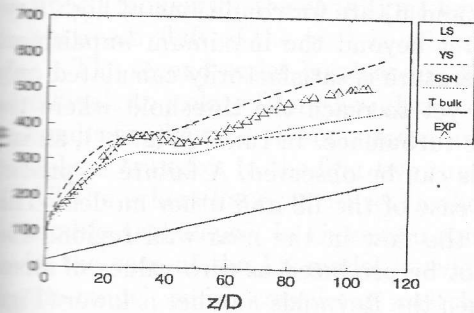
Fig. 11. Wall temperature development – simulation of experiment of Vilemas et al. – run 6.
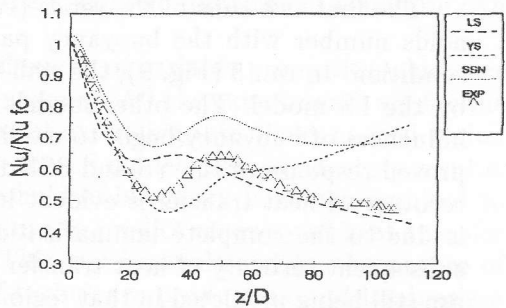
Fig. 12. Relative heat transfer development – run 6.
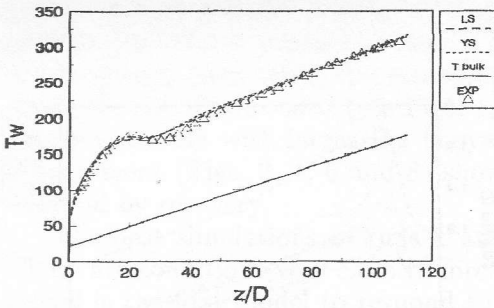
Fig. 13. Wall temperature development – simulation of experiment of Vilemas et al. – run 7.
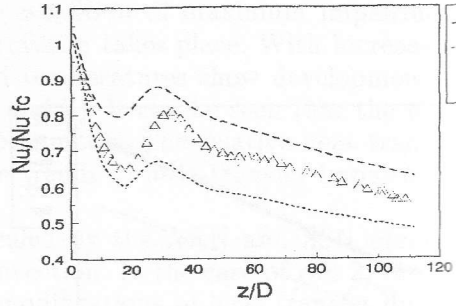
Fig. 14. Relative heat transfer development – run 7.
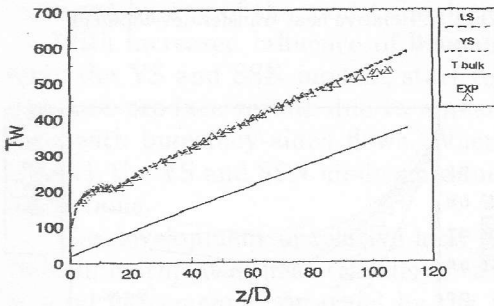
Fig. 15. Wall temperature development – simulation of experiment of Vilemas et al. – run 8.
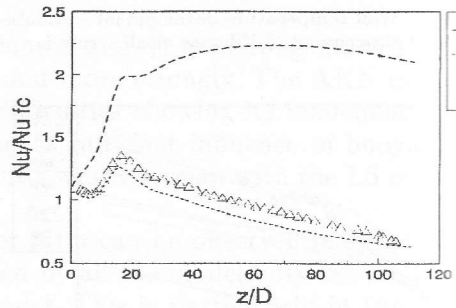
Fig. 16. Relative heat transfer development – run 8.

relative heat transfer plots (see Figs. 10, 12, 14 and 16) show the development impairment and subsequent enhancement (runs 3 and 4) of heat transfer.

The first two runs of the series (runs 5 and 6) are for conditions of high Reynolds number with the buoyancy parameter beyond the maximum impairment condition. In run 5 (Fig. 9), the wall temperature is satisfactorily calculated only by the LS model. The other models have yet to reach the threshold where influences of buoyancy begin to modify the turbulence. In run 6 (Fig. 11), an improved response of the YS and SSN models can be observed. A failure to predict recovery of heat transfer is evident in the case of the LS and other models. This is due to the complete laminarization of the flow in the near-wall region. The subsequent recovery of heat transfer cannot be produced as zero values of stress are still being predicted in that region. When the Reynolds number is lower (Figs. 13 and 15) the YS, LS and SSN models all respond to the combined effects of the buoyancy and variable properties. In these cases it seems that the LS and YS models give the same agreement with the experiment. It should be noted that with increase of buoyancy influence, the models encounter convergence problems and fail to complete calculations (AKN and eventually the SSN models). The

upstream shift of the peak of wall temperature is captured in the calculations. From the relative heat transfer distributions we can see that the agreement with the experiment is not as good as it was in the simulations discussed earlier. This can be associated with the effects of variable properties. It was found in [18] that all the models tend to over-predict this effect. In the present series the wall-to-bulk temperature differences are very high and therefore the kinematic viscosity undergoes large variations. We can expect, therefore, that variable property effect will be strongly over-predicted. The wall-to-bulk temperature difference in buoyancy-influenced ascending flow simulations is much greater than that found in the forced convection, and in the normalization procedure the difference in over-prediction of the variable property effect shows up. This is a main reason for the discrepancy between simulations and experiment in the normalized results. We can see that the LS model predictions start to depart from the experimental results. In the case of high buoyancy influence and high wall-to-bulk temperature differences this discrepancy increases. The YS and SSN models show similar disagreement with experiment but to a much smaller extent.

5. Concluding remarks

The experiments of Vilemas et al. are an important contribution to literature on ascending flow mixed convection. Prior to the present study no attempts have been to simulate these data using the kind of the models considered here.

In the first series of runs, where only small variable property effects are present, the best agreement with experiment in the impaired heat transfer region before maximum impairment is returned by the LS model. Beyond this condition (as was found earlier) the YS and SSN models start to respond more strongly to the influences of buoyancy and the SSN model seems to give the best agreement with experiment. Clear peaks on the wall temperature are calculated by the forementioned models for the conditions beyond the maximum impairment condition. An upstream shift of the peak is evident.

The second series involves marked influences of variable properties which are difficult to isolate from the influence of buoyancy. All the experiments are for the conditions beyond the maximum impairment extending into the enhanced region of heat transfer. In the first two runs only the LS model gives satisfactory results. All the others have yet to reach the threshold of buoyancy influence required to modify turbulence. In these two runs, failure to predict recovery of heat transfer in the case of the LS model is evident. This can be explained by the nature of the model, which completely switches off turbulence production and laminarizes the flow in the wall region. Subsequent recovery of heat transfer therefore cannot occur. In runs 7 and 8 the YS model starts to respond to the influences of buoyancy and gives almost identical simulations to those of the LS model.

The relative heat transfer plot is misleading in these cases, as the influence of variable properties is introducing a systematic shift of the results.

6. Conclusions

(a) For conditions of forced convection with negligible influences of buoyancy the models are well tuned to the experimental results.

(b) The effects of viscosity variation are over-predicted by most of the models considered here.

(c) The SSN and LS models clearly perform best in terms of reproducing the influences of buoyancy. The enhancement of heat transfer due to buoyancy is generally underestimated by the models. The AKN model does respond but fails to give results if the inlet conditions correspond to higher values of buoyancy parameter.

(d) When the flow is fully laminarised, the YS and LS models return exactly the same results.

(e) From the present study it seems that the form of parameter in the damping function of the $k \sim \epsilon$ turbulence models studied which is best able to respond to buoyancy influences is the local turbulent Reynolds number $Re_t = k^2/\nu\epsilon$. The Kolmogorov velocity scale $u_\epsilon = (\nu\epsilon)^{1/4}$ is an prospective parameter and ought to be examined in more detail.

(f) Overall, the LS, YS and SSN models perform best and will be scrutinised.

Acknowledgements

References

[1] Vilemas J.V., Poskas P.S. and Kaupas V.E.: *Local heat transfer in a vertical gas-cooled tube with turbulent mixed convection and different heat fluxes*, Int. J. Heat Mass Transfer, 35(1992), 2421-2428.

[2] Mikielewicz D.P.: *Comparative studies of turbulence models under conditions of mixed convection with variable properties in heated vertical tubes*, Ph.D. Thesis, University of Manchester, 1994.

[3] Cotton M.A.: *Theoretical studies of mixed convection in vertical tubes*, Ph.D. Thesis, University of Manchester, 1987.

[4] Yu L.S.L.: *Computational studies of mixed convection in vertical pipes*, Ph.D. Thesis, University of Manchester, 1991.

[5] Launder B.E. and Sharma B.I.: *Application of the energy-dissipation model of turbulence to the calculation of flow near a spinning disc*, Lett. Heat Mass Transfer, 1(1974), 131-138.

[6] Yang Z. and Shih T.H.: *New time scale based $k \sim \epsilon$ model for near-wall turbulence*, AIAA J., 31(1993), No. 7, 1191-1198.

[7] Abe K., Kondoh T. and Nagano Y.: *A new turbulence model for predicting fluid flow and heat transfer in separating and reattaching flows-I. Flow field calculations*, Int. J. Heat Mass Transfer, 37(1994), No. 1, 139-151.

[8] Sato H., Shimada M. and Nagano Y.: *A two-equation turbulence model for predicting heat transfer in various Prandtl number fluids*, Paper 3-NT-27, 10th Int. Heat Transfer Conf., Brighton, 1994.

[9] Mikielewicz D.P. and Ihnatowicz E. : *Turbulence modelling using various turbulent Prandtl number*, Transactions of IFFM, No. 100, 1996, 141-154.

[10] Cotton M.A. and Jackson J.D.: *Vertical tube air flows in the turbulent mixed convection regime calculated using a low-Reynolds-number $k \sim \epsilon$ model*, Int. J. Heat Mass Transfer, 33(1990), 275-286.

[11] Cotton M.A., Jackson J.D. and Yu L.S.L.: *Low-Reynolds-number $k \sim \epsilon$ simulations of turbulent mixed convection air flows in vertical pipes: inclusion of variable property effects*, submitted to Int. J. Heat Mass Transfer, 1995.

[12] Carr A.D., Connor M.A. and Buhr H.O.: *Velocity, temperature and turbulence measurements in air for pipe flow with combined free and forced convection*, J. Heat Transfer, 95(1973), 445-452.

[13] Steiner A.: *On the reverse transition of a turbulent flow under the action of buoyancy forces*, J. F. Mech., 47(1971), 503-512.

[14] Polyakov A.F. and Shindin S.A.: *Development of turbulent heat transfer over the length of vertical tubes in the presence of mixed air convection*, Int. J. Heat Mass Transfer, 31(1988).

[15] Petukhov B.S. and Kurganov V.A.: *Analysis and processing of heat transfer data in turbulent gas pipe flows with variable physical properties*, Teplofizika Vysokich Temperatur, 12(1974).

[16] Mikielewicz D. P.: *Modelling of a vertical pipe flow in forced convection*, Zeszyty Naukowe IMP PAN, 454/1410/95.

[17] Barnes J.F. and Jackson J.D.: *Heat transfer to air, carbon dioxide and helium flowing through smooth circular tubes under conditions of large surface/gas temperature ratio*, Journal Mechanical Engineering Science, 3(1961), 303-313.

[18] Mikielewicz D.P.: *Modelling a vertical pipe flow in descending flow of water*, Internal Report IMP PAN, No. 318/95, 1995, submitted to Archives of Thermodynamics.

[19] Hall W.B. and Jackson J.D.: *Laminarization of a turbulent pipe flow by buoyancy forces*, ASME Paper, 69-HT-55, 1969.

[20] Jackson J.D. and Hall W.B.: *Influences of buoyancy on heat transfer to fluids flowing in vertical tubes under turbulent conditions*, Turb. Forced Convection in Channels and Bundles, Theory and Application to Heat Exchanger and Nuclear Reactor, 2, Adv. Study Inst. Book (eds. Kakac S. and Spalding D.B.), 1979.

Modelowanie przepływu wznoszącego powietrza w pionowej grzanej rurze

Streszczenie

W niniejszej pracy przedstawiono wyniki bezpośrednich porównań symulacji numerycznych przy użyciu modeli turbulencji z grupy $k \sim \epsilon$ z danymi eksperymentalnymi dotyczącymi przepływu wznoszącego powietrza w grzanej pionowej rurze. Symulacje przeprowadzone były przy uwzględnieniu zmienności własnosci fizycznych płynu. Obliczenia przeprowadzono przy założeniu stałej liczby turbulentnej Prandtla wynoszącej 0.85. Otrzymane wyniki obliczeń przy pomocy rozważanych modeli turbulencji należy uznać za satysfakcjonujące. Modele Sato, Shimady i Nagano oraz Laundera i Sharmy pokazały najlepszą zgodność z danymi eksperymentalnymi.